Hindawi
Modelling and Simulation in Engineering
Volume 2019, Article ID 9629643, 6 pages
https://doi.org/10.1155/2019/9629643

Research Article

Modeling and Simulation in Engineering Modeling of the Electrocoagulation Processes in Nonisothermal Conditions

Andrii Safonyk and Olena Prysiazhniuk

Department of Automation, Electrical Engineering and Computer-Integrated Technologies, National University of Water and Environmental Engineering, Rivne 33028, Ukraine

Correspondence should be addressed to Andrii Safonyk; safonik@ukr.net

Received 6 April 2019; Revised 14 September 2019; Accepted 10 October 2019; Published 3 November 2019

Academic Editor: Jing-song Hong

The paper suggests an approach to modeling the electrocoagulation process that is based on the generalization of the equations of incompressible fluid flow in nonisothermal conditions. In the model was taking into account the ratio between the values of the parameters which characterize the domination of convective and mass-exchange components of the process over diffusion. An asymptotic approximation of solutions of corresponding boundary value problems is constructed. Based on the received solutions, we conducted a computer simulation of the process of distribution of iron concentration inside the reactor that allows predicting various hydrodynamic phenomena such as internal recirculation and dead zones that affect the formation of a coagulant. The influence of current strength on the concentration of the target component at the exit from the reactor was investigated using the developed mathematical model. In addition, our findings also show the effect of the rate of heat formation from the electrodes on the efficiency of obtaining of coagulant.

1. Introduction

Reducing the volume of discharges of pollutants to the water reservoirs and transition of enterprises to work according to the scheme of the closed cycle of water use is the main direction of protection of the water environment. For the treatment of sewage of textile production, the reagent method is most often used.

It requires the use of a significant number of additional chemicals, one of which is divalent iron. Different technologies are used for its receipt, but the most resource-saving is electrocoagulation. This method has several advantages, such as versatility, absence of additional saline water pollution in the process of purification, small size and compactness of installations, ease of management, no need for reagents, easy maintenance of the equipment, weak sensitivity to changes in the conditions of the process, and obtaining sludge with better structural and mechanical properties. Among the main reasons hindering the widespread introduction of electrocoagulation into production are the technological complexity of the process and relatively high cost of electricity. In this regard, the actual direction of scientific research is the development of electrocoagulation technology for wastewater treatment, which will allow the creation of small-waste closed-end systems of water consumption at the enterprise and will be environmentally safe and economically feasible.

At present, many scientific studies are devoted to the simulation of electrocoagulation wastewater treatment [1–3]. However, the proposed mathematical models generally do not describe the kinetics of the process inside the electrocoagulator or do not take into account a number of parameters, for example, the effect of stomp force and changes in water temperature on the rate of flow of the process.

It is necessary to create source-saving technologies for water purification. Therefore, the purpose of this work is to develop a mathematical model of electrocoagulation processing which takes into account the process of formation of divalent iron from a solution of the electrolyte, the influence of technical characteristics (current strength, flow rate, inlet concentration of suspended particles, and temperature) on the kinetics of the process of mass and heat transfer in the electrocoagulation installation, and also the study of the influence of these parameters on the efficiency of the formation of a coagulant.

This method of sewage treatment is based on electrolysis which uses metal anodes which are exposed to electrolytic dissolution. As a result of the dissolution of the anodes, the water is enriched with the corresponding ions, forming in the neutral or low-alkaline medium, the hydroxide of iron. Flakes of hydroxides of metal collide with gas bubbles, connect with them, and expose them to the surface of the liquid after which they are separated mechanically. The electrocoagulation efficiency is influenced by the material of the electrodes, the distance between them, the velocity of the water flow between the electrodes, the temperature and composition of the water, the voltage, and the current density. The application of electrochemical methods is advisable at relatively high electrical conductivity of sewage due to the presence of inorganic acids, alkalis, or salts in them (with a minimum concentration of salts equal to 0.5 g/l).

1.1. Statement of the Problem.

Modeling of processes is executed based on equations which describe the motion of an incompressible fluid between the electrodes. The structure of the flow in the electrocoagulation installation (see Figure 1) can be either laminar or turbulent. In complex geometry, the speed field includes a random turbulent component that generates streams and turbulent vortices.

Continuous flow equations include equations of fluid dynamics, mass, pulse, and energy and provide a basis for modeling the process. These equations have many common features, so that a common variable can be used to describe the traditional forms of fluid flow equations, including scalar quantities such as temperature and concentration. This general equation is written in the following form [3]:

$$\frac{\partial(\rho Q)}{\partial t} + \nabla(\rho v Q) = \nabla\left(D_Q \nabla Q\right) + S_Q, \tag{1}$$

where the variable Q may be the velocity in the direction x, y, and z, temperature, or concentration; ρ is liquid density, kg/m^3; v is average velocity vector; D_Q is diffusion coefficient, m^2/s; and S_Q is source of temperature or concentration. For electrochemical systems, equation (1) is simplified through the equation of mass continuity and the Navier–Stokes equation [4].

The basic equations for an incompressible turbulent flow can be formulated as follows [5]:

$$\rho(v\nabla)v = -\nabla P + \nabla\left(\left(\mu + \mu_T\right)\left(\nabla v + (\nabla v)^T\right)\right), \tag{2}$$

$$\nabla(\rho v) = 0, \tag{3}$$

where P is pressure, Pa, and μ is dynamic viscosity, Pa·s. The Reynolds stress can be expressed in terms of turbulent viscosity μ_T according to the standard model [6].

In a nonisothermal turbulent flow for the case when density and thermal conductivity are constant values, applying the averaging rule to the heat equation, we obtain [7–9]

$$\frac{\partial T}{\partial t} + (v \cdot \nabla)T = a\nabla^2 T + \frac{q_V}{\rho c_\rho}, \tag{4}$$

where $a = k/\rho c_\rho$ is thermal diffusivity, m^2/s; k is thermal conductivity, W/(m·K); c_ρ is specific heat capacity, J/(kg·K); ρ is density, kg/m^3; and q_V is the intensity of internal heat sources, W/m^3. The amount of heat released during the electrode heating of the liquid is proportional to the current strength, and its time of passage and the voltage drop is $q_v = I \cdot U \cdot t$, where U is applied voltage, V, and I is current, A.

The change in concentration C is described by means of the scalar transport equation with the contributions of turbulent [10]:

$$\frac{\partial C}{\partial t} = -v\nabla C + \nabla(D\nabla C) + S_C, \tag{5}$$

where $D = \overline{D} + D_{\text{turb}}$ is the total diffusion coefficient, $\overline{D}$ is the coefficient of molecular diffusion, and D_{turb} is the coefficient of turbulent diffusion, which depends on and the Schmidt turbulent number Sc_T (according to the Kays–Crawford model [5]).

The effectiveness of the formation of flocs (coagulant) to a large extent depends on the size of the formed bubbles [11]. Electroflotation produces a large number of fine gas bubbles, the size of which varies from 5 to 90 μm depending on the state of electrolysis. Smaller bubble sizes create the best kinetics of flotation due to the high ratio of surface area to volume. Furthermore, small bubbles are more likely to get smaller contact angle in the system for three-phase (gas-liquid-solid) than larger bubbles. The smaller contact angle produces more stable units. In addition, the time of detention of small bubbles in the flotation unit is longer than the time of the detention of larger bubbles, since they have a lower velocity. This contributes to increase the probability of collision of gas bubbles and flocs. Conversely, the shear forces of the larger bubbles are high due to the high velocity of motion, which can cause the floc to break.

In [12], deposition of Brownian particles to hydrogen bubbles is described. The velocity of the flotation component of the electroflotation process is quantified as follows:

$$\frac{\partial C}{\partial t} = \left(\eta \frac{3R_g T I}{8F d_b A_s p_a}\right) C, \tag{6}$$

where R_g is ideal gas constant, p_a is its atmospheric pressure, A_s is cross-sectional area of the chamber, and η is efficiency of accumulation with one bubble which is defined as the proportion of the pollutant in the path of the bubble that actually adheres to the bubble. In [13], numerical expressions are also proposed for the calculation of η.

Thus, in order to find the distribution of the coagulant concentration C and temperature T in the electrocoagulator we obtained the system of two questions:

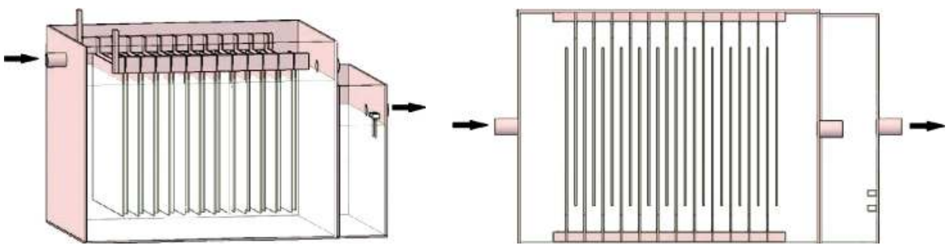

(a)

(b)

Figure 1: Scheme of electrocoagulation installation.

$$\begin{cases} \dfrac{\partial C}{\partial t} = -v\nabla C + \nabla\left(D(T)\nabla C\right) + \left(\eta\dfrac{3R_gTI}{8Fd_bA_sp_a}\right)C, \\ \\ \dfrac{\partial T}{\partial t} + (v\cdot\nabla)T = a\nabla^2T + \dfrac{IUt}{\rho c_\rho}, \end{cases} \tag{7}$$

with the following conditions:

$$\begin{aligned} & C(x,y,0) = C_0(x,y), \\ & T(x,y,0) = T_0(x,y), \\ & C(0,y,t) = C_*(y,t), \\ & T(0,y,t) = T_*(y,t), \\ & C(L,y,t) = C^*(y,t), \\ & T(L,y,t) = T^*(y,t), \\ & \left.\frac{\partial C}{\partial y}\right|_{y=0} = 0, \\ & \left.\frac{\partial C}{\partial y}\right|_{y=y^*} = 0, \\ & \left.\frac{\partial T}{\partial y}\right|_{y=0} = -\alpha\left(T(x,0,t) - T_*^*\right), \\ & \left.\frac{\partial T}{\partial y}\right|_{y=y^*} = -\alpha\left(T(x,y^*,t) - T_*^*\right). \end{aligned} \tag{8}$$

2. Methods

Taking into account the relationship between the values of parameters that characterize certain components of the process (in particular the dominance of convective and mass-exchange factors over diffusion) leads to the complication of the mathematical model of the process. These singularities are generated by the presence of small parameters. One of the effective ways of solving the corresponding problems in the case of the predominance of convective factors of the process over diffusion during filtration of aqueous solutions in the model regions limited by equipotential or quasi-equipotential lines and flow lines is as follows: phased fixation of the characteristics and components of the process and environment; solving filtration problems using conformal or quasi-conformal mappings of a complex potential or quasi-potential area on a physical area; and transition in equations of convective diffusion and boundary and initial conditions from physical variables to the coordinates of the region of complex potential or quasi-potential, which greatly simplifies their recording and provides the possibility of autonomous research, parallel computing.

Taking into account that the problem is to find the velocity field (2) and (3) with the given boundary conditions [5] is resolved [12], in particular, calculated velocity field and a number of other variables, such as filtration consumption, and replaced the variables $x = x(\varphi,\psi)$, $y = y(\varphi,\psi)$ in the system (7) and conditions (8), the corresponding "diffusion problem" [14, 15] was received. The solutions with precision $O(\delta^{n+1})$ (δ -small parameter characterizing the predominance of the convective and mass-exchange components of the process of mass transfer, $D(T) = \delta\, d(T)$, $|v| > v_* \gg \delta$) was found in the form of asymptotic series [16]:

$$\begin{aligned} C(\varphi,\psi,t) = {} & \sum_{i=0}^{n}\delta^i C_i(\varphi,\psi,t) + \sum_{i=0}^{n+1}\delta^i\overline{C}_i(\xi,\psi,t) \\ & + \sum_{i=0}^{2n+1}\delta^{i/2}\underset{\frown}{C}_i(\varphi,\zeta,t) + \sum_{i=0}^{2n+1}\delta^{i/2}\breve{C}_i(\varphi,\phi,t) \\ & + R_C(\varphi,\psi,t,\delta), \end{aligned} \tag{9}$$

$$\begin{aligned} T(\varphi,\psi,t) = {} & \sum_{i=0}^{n}\delta^i T_i(\varphi,\psi,t) + \sum_{i=0}^{n+1}\delta^i\overline{T}_i(\xi,\psi,t) \\ & + \sum_{i=0}^{2n+1}\delta^{i/2}\underset{\frown}{T}_i(\varphi,\zeta,t) + \sum_{i=0}^{2n+1}\delta^{i/2}\breve{T}_i(\varphi,\phi,t) \\ & + R_T(\varphi,\psi,t,\delta), \end{aligned} \tag{10}$$

where R_C and R_T are residual members of the schedules, $C_i(\varphi,\psi,t)$ and $T_i(\varphi,\psi,t)$ are regular parts of the asymptotic series, $\overline{C}_i(\xi,\psi,t)$ and $\overline{T}_i(\xi,\psi,t)$ are functions of the type of adjoining layer at the output of the filtration flow from the region, $\underset{\frown}{C}_i(\varphi,\zeta,t)$, $\underset{\frown}{T}_i(\varphi,\zeta,t)$, $\breve{C}_i(\varphi,\phi,t)$, and $\breve{T}_i(\varphi,\phi,t)$ are functions of the type of adjoining layer in the windows of the side walls of the electrocoagulation installation, and

$\xi = (L - x) \cdot \delta^{-1}$, $\zeta = y \cdot \delta^{-1/2}$, and $\phi = (y^* - y) \cdot \delta^{-1/2}$ are corresponding regularizing transformations.

Expressions for regular parts of the asymptotic solutions are found as a result of applying the procedure of substitution of the series (9) and (10) and the equation of coefficients for the same powers of the small parameter and solving the corresponding problems:

$$T_i(\varphi,\psi,t) = \begin{cases} \displaystyle\int_0^t \widetilde{T}_i\left(f^{-1}(\tilde{t} - t + f(\varphi,\psi),\psi),\tilde{t}\right)\mathrm{d}\tilde{t} + \tau^*_{*i}(\varphi,\psi), & t \le f(\varphi,\psi), \\ \displaystyle\int_{\varphi_*}^{\varphi} \frac{\widetilde{T}_i(\tilde{\varphi}, f(\tilde{\varphi},\psi) + t - f(\varphi,\psi))}{v(\tilde{\varphi},\psi)}\mathrm{d}\tilde{\varphi} + \tau_i^*(\varphi,\psi), & t > f(\varphi,\psi),\ i = \overline{0,n}, \end{cases}$$

$$C_0(\varphi,\psi,t) = \begin{cases} e^{\int_{\varphi^*}^{\varphi}\left(g_0(\tilde{\varphi},f(\tilde{\varphi},\psi)-f(\varphi,\psi)+t)\right)/(v(\tilde{\varphi},\psi))\mathrm{d}\tilde{x}}\, C_0(t - f(\varphi,\psi)), & t > f(\varphi,\psi), \\ e^{\int_0^t g_0\left(f^{-1}(\tilde{t}+f(\varphi,\psi)-t),\psi,\tilde{t}\right)\mathrm{d}\tilde{t}}\, C_*(f^{-1}(f(\varphi,\psi) - t,\psi)), & t \le f(\varphi,\psi), \end{cases}$$

$$C_i(\varphi,\psi,t) = \begin{cases} e^{\int_{\varphi_*}^{\varphi}\left(g_i(\varphi,\psi,f(\tilde{\varphi},\psi)-f(\varphi,\psi)+t)\right)/(v(\tilde{\varphi},\psi))\mathrm{d}\tilde{x}} \displaystyle\int_{\varphi_*}^{\varphi} \frac{h_i(\varphi,\psi,f(\tilde{\varphi},\psi) - f(\varphi,\psi) + t)}{v(\tilde{\varphi},\psi)} & \\ \quad \times e^{-\int_{\varphi_*}^{\varphi}\left(g_i(\tilde{\tilde{\varphi}},\psi,f(\tilde{\tilde{\varphi}},\psi)-f(\tilde{\varphi},\psi)+t)\mathrm{d}\tilde{\tilde{\varphi}}\right)/(v(\tilde{\tilde{\varphi}},\psi))}\mathrm{d}\tilde{\varphi}, & t > f(\varphi,\psi), \\ e^{\int_0^t g_i\left(f^{-1}(\tilde{t}+f(\varphi,\psi)-t,\psi),\tilde{t}\right)\mathrm{d}\tilde{t}} \displaystyle\int_0^t h_i\left(f^{-1}(\tilde{t} + f(\varphi,\psi) - t,\psi),\tilde{t}\right) e^{-\int_0^{\tilde{t}} g_i\left(f^{-1}(\tilde{\tilde{t}}+f(x)-t,\psi),\tilde{\tilde{t}}\right)\mathrm{d}\tilde{\tilde{t}}}\mathrm{d}\tilde{t}, & t \le f(\varphi,\psi),\ i = \overline{1,n}, \end{cases} \tag{11}$$

where $f(\varphi,\psi) = \int_{\varphi_*}^{\varphi} (\mathrm{d}\tilde{\varphi})/(v(\tilde{\varphi},\psi))$, $\widetilde{T}_0(\varphi,\psi,t) = (IUt/c\rho)$, $\tau_0^*(\varphi,\psi) = \mathrm{T}^*(f^{-1}(f(\varphi,\psi) - t,\psi))$, $\tau^*_{*0}(\varphi,\psi) = T_0(t - f(\varphi,\psi),\psi)$, $\widetilde{T}_i(\varphi,\psi,t) = \overline{d}_T((\partial^2 T_{i-1}/\partial\varphi^2) + (\partial^2 T_{i-1}/\partial\psi^2))$, $\overline{d}_T = a\lambda_m/\delta\lambda$, $\tau_i^*(\varphi,\psi) = \tau^*_{*i}(\varphi,\psi) = 0 \cdot (i = \overline{1,n})$, $g_i(\varphi,\psi,t) = \eta(3R_g I T_i(\varphi,\psi,t))/(8Fd_b A_s P)$, $h_i(\varphi,\psi,t) = \overline{d}_{iC}((\partial^2 C_{i-1}/\partial\varphi^2) + (\partial^2 C_{i-1}/\partial\psi^2))$, and $\overline{d}_{iC}$ are known functions that are the sum of the products of the members of the series (9) and (10), their partial derivatives, and the coefficients of the corresponding powers of the small parameter in the decomposition of the corresponding functions $d(L - \xi\delta,\psi,t)$ in the Taylor series in the vicinity $\varphi = L$. Functions of the type of adjoining layer are found similarly to [14–16].

3. Results of Numerical Calculations

The computer simulation was carried out at the following values of the parameters $\eta = 0.8$, $c = 3.31 \cdot 10^3$ J/kg, $\rho = 1060$ kg/m^3, $\lambda = 0.2$ W/(m·s), $a = 1.39 \cdot 10^{-8}$ m^2/s, $R_g = 8.31$ J/(mol·K), $F = 9.65 \cdot 10^4$ C/mol, $A_s = 15$ m^2, $d_b = 1.5 \cdot 10^{-6}$ m, $D = 10^{-9}$ m^2/s, and $T_*^* = 294$ K. Provided that the current strength is equal to 70 A, the concentration of iron ions at the exit from the electrocoagulator is obtained 16.5 mg/l at moments of 90 minutes, 68.4 mg/l at 180 min, and 101.8 mg/l at 240 min [2]. The results of the experiment and the calculation of the model problem (7) and (8) are presented in Figure 2.

In practice, current is the only operating parameter after other operating parameters such as pH, volume flow of water, and design dimensions of the reactor and others are regulated, which affects the kinetics of the coagulant formation process. The distribution of the concentration of iron and water temperature in the electrocoagulation installation at the initial time and after 240 min is shown in Figures 3 and 4. As expected, the concentration of iron increases in the space between the electrodes, which conventionally wears out to the exit of the electrocoagulation installation, where its concentration is highest. Similarly, the temperature of the electrolyte increases uniformly along the length of the electrocoagulation installation, and due to the convective transfer of the entrance to the cold water and cooling by the walls, we obtain the maximum temperature values near the electrodes and at the outlet of the electrocoagulation installation (Figure 4).

Analysis of the distribution of iron concentration inside the reactor allows predicting various hydrodynamic phenomena such as internal recirculation and dead zones that affect the formation of a coagulant.

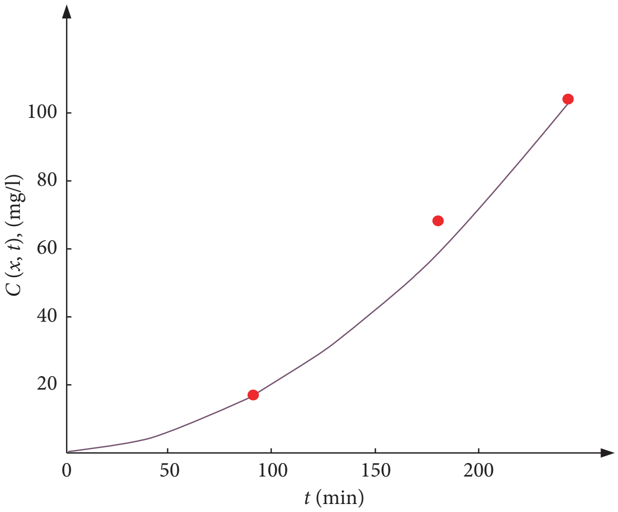

Figure 2: Distribution of the concentration of divalent iron over time at the exit of the coagulator.

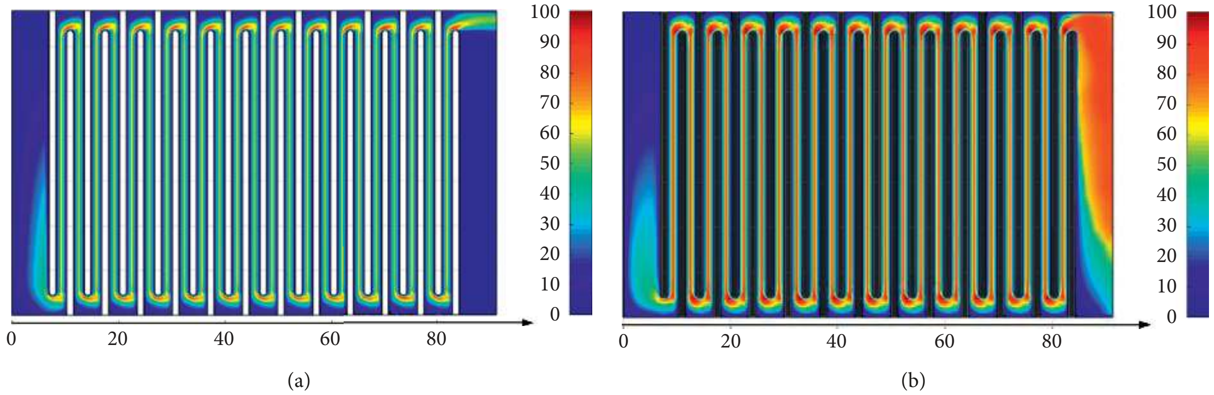

(a)

(b)

Figure 3: The distribution of the concentration of iron at the initial time (a) and after 240 min (b).

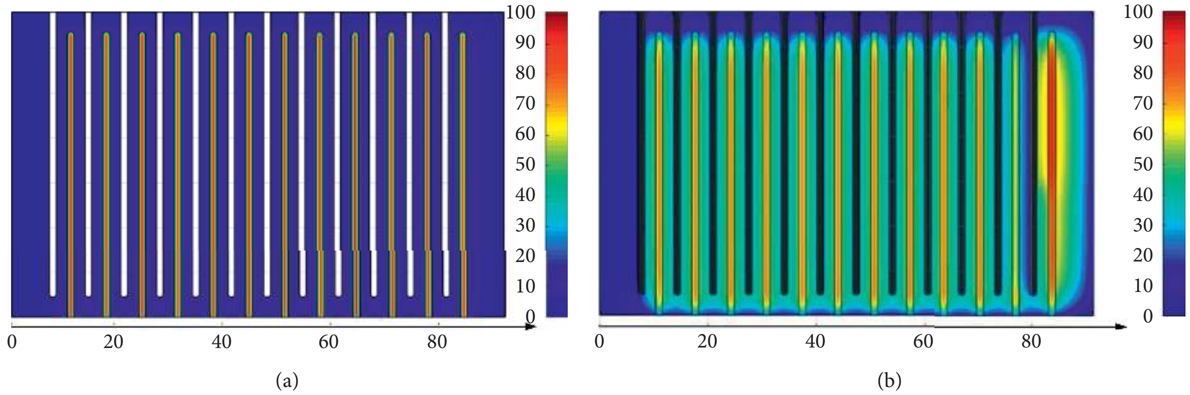

(a)

(b)

Figure 4: The distribution of the water temperature at the initial time (a) and after 240 min (b).

4. Conclusions

A mathematical model describing the laws of the course of heat and mass transfer processes in an electrocoagulation plant was developed. The solution of the corresponding model problem with the use of the asymptotic approximation of the solution of the boundary value problem is found, and the results of calculations of the distribution of the concentration of iron and water temperature in the electrocoagulation installation and the output of the coagulator depending on the current strength are given. The proposed methodology for calculating the concentration distribution can be used to analyze the influence of heat and mass transfer in the electrolyte and the kinetics of the reaction on the electrodes, as well as the basis for experimental and theoretical studies of optimization and automation of the process of formation of coagulant by the method of electrocoagulation.

Data Availability

Previously reported experimental data were used to support this study and are available at DOI: 10.1109/STC-CSIT.2018.8526661. These prior studies (and datasets) are cited at relevant places within the text as references [2].

Conflicts of Interest

The authors declare that there are no conflicts of interest regarding the publication of this paper.

References

[1] J. N. Hakizimana, B. Gourich, M. Chafi et al., "Electrocoagulation process in water treatment: a review of electrocoagulation modeling approaches," *Desalination*, vol. 404, pp. 1–21, 2017.

[2] A. Safonyk, A. Bomba, and I. Tarhonii, "Modeling and automation of the electrocoagulation process in water treatment," *Advances in Intelligent Systems and Computing*, vol. 871, pp. 451–463, 2018.

[3] V. Khandegar and A. K. Saroha, "Electrocoagulation for the treatment of textile industry effluent - a review," *Journal of Environmental Management*, vol. 128, pp. 949–963, 2013.

[4] H. Versteeg and W. Malalasekera, *An Introduction to Computational Fluid Dynamics: The Finite Volume Method*, Vol. 503, Pearson Education, London, UK, 2007.

[5] M. A. Sandoval, R. Fuentes, F. C. Walsh, J. L. Nava, and C. P. de León, "Computational fluid dynamics simulations of single-phase flow in a filter-press flow reactor having a stack of three cells," *Electrochimica Acta*, vol. 216, pp. 490–498, 2016.

[6] R. Enciso, L. Padilla, C. Ojeda et al., "Computational fluid dynamics characterization of a rotating cylinder electrochemical reactor using an RANS-RNG turbulence model," *International Journal of Electrochemical Science*, vol. 7, pp. 12181–12192, 2012.

[7] V. Kulinchenko and S. Tkachenko, "Heat-transfer with elements of mass-transfer (theory and practice of process)," *Feniks*, pp. 1–917, 2014.

[8] A. P. Vlasyuk and V. V. Zhukovskii, "Mathematical simulation of the migration of radionuclides in a soil medium under nonisothermal conditions with account for catalytic microparticles and nonlinear processes," *Journal of Engineering Physics and Thermophysics*, vol. 90, no. 6, pp. 1386–1398, 2017.

[9] P. M. Martyniuk, M. T. Kuzlo, S. K. Matus, and T. P. Tsvietkova, "Mathematical model of nonisothermal moisture transference in the form of water and vapor in soils in the case of chemical internal erosion," *Far East Journal of Mathematical Sciences (FJMS)*, vol. 102, no. 12, pp. 3211–3221, 2017.

[10] A. S. Naje, S. Chelliapan, Z. Zakaria, M. A. Ajeel, and P. A. Alaba, "A review of electrocoagulation technology for the treatment of textile wastewater," *Reviews in Chemical Engineering*, vol. 33, pp. 263–292, 2017.

[11] R. Alam and J. Q. Shang, "Electrochemical model of electroflotation," *Journal of Water Process Engineering*, vol. 12, pp. 78–88, 2016.

[12] X. Chen and G. Chen, "Electro-flotation," in *Electrochemistry for the Environment*, C. Comninellis and G. Chen, Eds., pp. 263–277, Springer Science + Business Media, LLC, Berlin, Germany, 2010.

[13] Y. Fukui and S. Yuu, "Collection of submicron particles in electro-flotation," *Chemical Engineering Science*, vol. 35, no. 5, pp. 1097–1105, 1980.

[14] A. Safonyk, S. Martynov, S. Kunytsky, and O. Pinchuk, "Mathematical modelling of regeneration the filtering media bed of granular filters," *Advances in Modelling and Analysis C*, vol. 73, no. 2, pp. 72–78, 2018.

[15] A. Y. Bomba and A. P. Safonik, "Mathematical simulation of the process of aerobic treatment of wastewater under conditions of diffusion and mass transfer perturbations," *Journal of Engineering Physics and Thermophysics*, vol. 91, no. 2, pp. 318–323, 2018.

[16] A. Bomba, Y. Klymiuk, I. Prysiazhniuk, O. Prysiazhniuk, and A. Safonyk, "Mathematical modeling of wastewater treatment from multicomponent pollution by using microporous particles," *AIP Conference Proceedings*, vol. 1773, pp. 1–11, 2016.


Journal of
Engineering

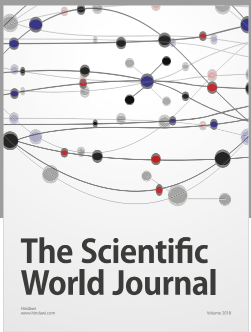
The Scientific
World Journal

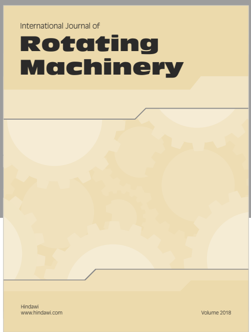
International Journal of
Rotating
Machinery


Journal of
Sensors

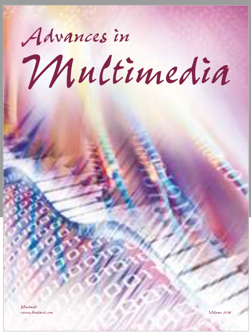
Advances in
Multimedia

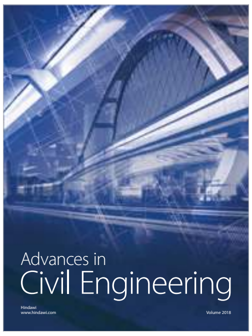
Advances in
Civil Engineering

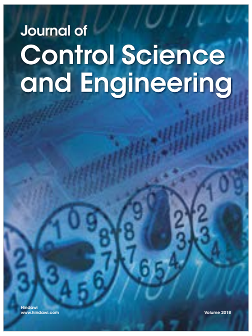
Journal of
Control Science
and Engineering


Journal of
Robotics


Journal of
Electrical and Computer
Engineering

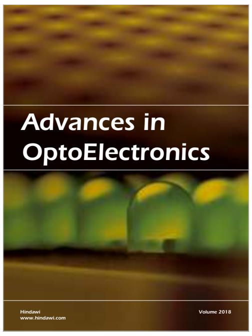
Advances in
OptoElectronics


VLSI Design


International Journal of
Navigation and
Observation

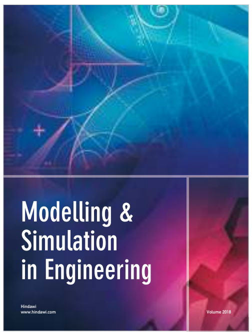
Modelling &
Simulation
in Engineering


International Journal of
Aerospace
Engineering


International Journal of
Chemical Engineering

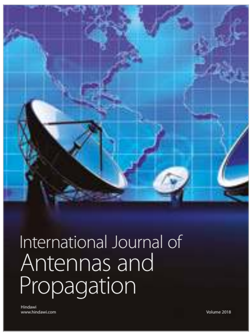
International Journal of
Antennas and
Propagation


Active and Passive
Electronic Components

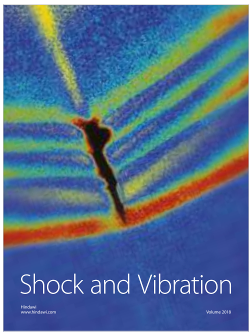
Shock and Vibration

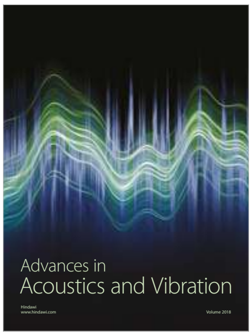
Advances in
Acoustics and Vibration